Optimisation Of MHD Stability Using ECCD In ASDEX Upgrade

A. Manini[1], M. Maraschek[1], S. Cirant[2], G. Gantenbein[3], F. Leuterer[1], H. Zohm[1] and the ASDEX Upgrade Team[1]

[1]*Max-Planck-Institut für Plasmaphysik, EURATOM Association, 85748 Garching, Germany*
[2]*Associazione EURATOM-ENEA sulla Fusione, IFP-CNR, Milano, Italy*
[3]*Forschungszentrum Karlsruhe, PO Box 3640, 76021 Karlsruhe, Germany*

Abstract. The active control of core MHD activity in fusion plasmas plays a very important role for increasing the performance of a reactor. Recently, in ASDEX Upgrade, a significant effort has been made to optimise the control of MHD stability using its ECRH system, in particular of sawteeth and NTMs. The sawtooth stability depends on the local shear at q=1, which can be modified by local on/off-axis co-/ctr-ECCD around q=1. The effects on the sawtooth period between wide and narrow CD widths are compared. The strongest effects occur in co-ECCD and with narrow CD width. The effects of ctr-ECCD with wide deposition are dominated by the heating, while the ones with narrow deposition by the CD contribution. Comparison of scans in co-/ctr-ECCD and pure ECRH shows that the CD effects contribute linearly to the modifications of the sawtooth period. Normally, NTMs appear in plasmas with high normalised pressure $\beta_N = \beta_t/(I_p/aB_T)$. The flattening of the pressure profile within the magnetic island leads to a hole in the bootstrap current profile, hence to a reduction of the plasma performance. Once NTMs are excited, they can be fully stabilised at high β_N with co-ECCD at the resonant surface. Experiments on the dependence of the control of NTMs on the ECCD deposition width and on the total driven current are presented, together with NTM stabilisation studies using modulated and non-modulated ECCD. By reducing the CD width, the stabilisation efficiency is significantly improved. Full NTM stabilisation with narrow ECCD width is obtained at higher β_N than before. Full NTM stabilisation with wide CD width is obtained with modulated ECCD in conditions in which non-modulated ECCD does not completely stabilise.

Email of A. Manini: adriano.manini@ipp.mpg.de

INTRODUCTION

Core magneto-hydro-dynamic (MHD) activity, such as sawteeth and neoclassical tearing modes (NTM), is of general interest for the overall performance of fusion experiments and in particular for ITER and later fusion reactors. The sawtooth activity in tokamak plasmas plays a very important role in the determination of both plasma performance and profiles. The presence of sawteeth has the favourable effect of allowing the removal of impurities from the plasma core, particularly important in the presence of helium ash in a future reactor. On the other hand, sawtooth stabilisation produces centrally peaked temperature and density profiles, which are favourable for increasing the fusion yield. Long sawtooth periods (τ_{ST}) can lead to negative consequences, such as the creation of magnetic seed islands capable of triggering

neoclassical tearing modes (NTMs) [1]. The presence of a significant central fast ion population can transiently stabilise the internal kink modes [2], leading, as a consequence, to very long τ_{ST}. Since plasma performance and fusion yield have opposite dependence on τ_{ST}, an optimised period length should be identified in order to maximise both. On the other hand, NTMs appear only in discharges with high normalised pressure $\beta_N = \beta_t / (I_P / aB_T)$. The flattening of the pressure profile within the island (due to high parallel heat transport) leads to a hole in the bootstrap current profile, which is the main drive for a NTM. A (3/2)-NTM reduces the achievable β by at least 10-20%. Since for the fusion power $P_{fus} \propto \beta^2$ holds, such loss is not acceptable for a fusion reactor. A (2/1)-NTM leads to a larger confinement loss and the occurrence of a mode locking may even cause disruptions for low values of q_{95}.

For these reasons, it is essential to develop methods for controlling the MHD stability, and electron cyclotron resonance heating (ECRH) is particularly well suited for this purpose, because it is able to locally deposit very high power densities and to drive current (ECCD).

SAWTOOTH CONTROL OPTIMISATION

During recent years, several experiments have been performed to highlight the effects of ECRH and ECCD on the sawtooth period, in particular in TCV [3-5]. These experiments have motivated a set of related simulations, based on [2], with a sawtooth period model included in a transport code. The aim was to identify the separate effects of localised heating and CD in the stabilisation (τ_{ST} increases) and destabilisation (τ_{ST} decreases) of the sawteeth. The outcome of this work [6] is very important for the interpretation of the results presented below. First, it has been shown that the most efficient locations for stabilisation and destabilisation with pure localised heating are outside and inside the $q=1$ surface respectively. In particular, the simulations have shown that the heating location maximising τ_{ST} in radial scans of power deposition is closer to $q=1$ for a narrow deposition width as compared to a wide one. Consistently with experimental observations, the model showed that co- and ctr-ECCD have opposite effects at same radial locations with respect to the $q=1$ surface: inside $q=1$ ctr-ECCD is stabilising, whereas co-ECCD is destabilising; outside $q=1$ ctr-ECCD is destabilising, whereas co-ECCD is stabilising. Pure heating has the same effects as co-ECCD, therefore in the experiments the anti-symmetry breaks and the most efficient effects are obtained with co-ECCD outside and inside $q=1$ respectively [6]. In addition, the simulations showed that the magnetic shear at $q=1$ is the driving parameter in determining τ_{ST} and, in particular, the modification of the speed at which it increases during the sawtooth ramp before reaching the critical shear and the crash is triggered.

Sawtooth tailoring has been extensively investigated in ASDEX Upgrade H-modes heated by neutral beam injection (NBI) [7]. The results showed the possibility of both stabilisation or destabilisation with ECCD when the power is deposited at the right position close to $q=1$. However, these experiments have been conducted at constant toroidal launching angles $\phi_{tor} = \pm 15°$ for ECCD, which maximise the total driven current I_{CD} through the Doppler broadening of the deposition widths, as shown in

figure 1. As the magnetic shear at $q=1$ is the key element for the sawtooth stability [2, 6], the local ECCD current density j_{CD} is expected to play the key role, rather than I_{CD}. Therefore, new experiments have been performed to search for the optimum conditions for sawtooth tailoring by reducing ϕ_{tor} in order to maximise j_{CD} and, as a consequence, to minimise the power demand for an optimal control. Hence, $\phi_{tor}=\pm 6°$, for which j_{CD} is maximised (see figure 1), was chosen.

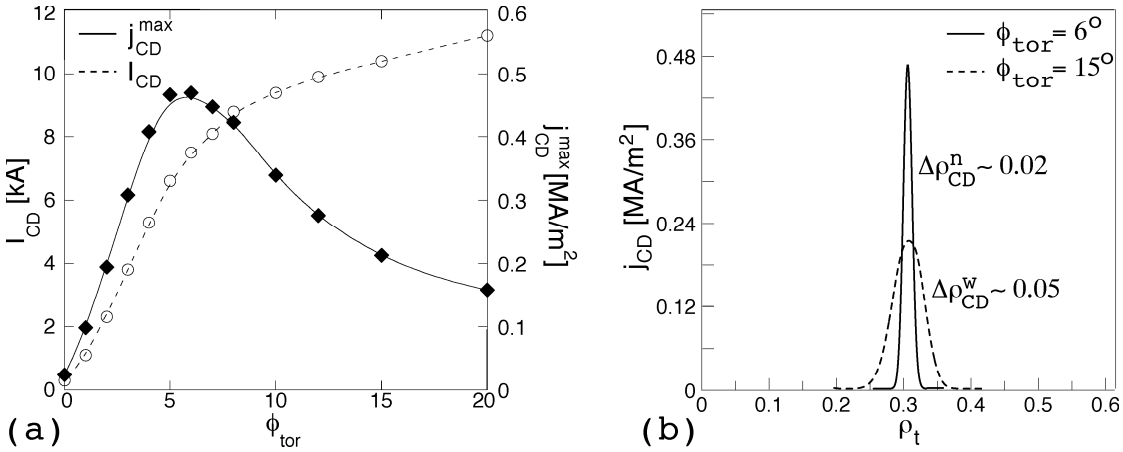

FIGURE 1. (a) Total driven current I_{CD} and maximum local driven current density j_{CD} as a function of the toroidal angle ϕ_{tor} with P_{ECCD}=700kW. (b) Driven current density profiles calculated with TORBEAM for ϕ_{tor}=6º,15º, i.e. narrow and wide deposition.

In order to investigate the dependence of τ_{ST} on the locally driven current density j_{CD} and on total driven current I_{CD}, a series of NBI-heated H-mode discharges similar to those described in [7] have been performed. The main parameters for these plasmas are: $I_P=800\,kA$, $n_e=6.0\cdot 10^{19}\,m^{-3}$, $q_{95}=4.5$, $\kappa=1.7$ $\delta=0.16$, $P_{NBI}=5\,MW$. The ECCD location, in both co- and ctr-ECCD, was scanned across $q=1$ by ramping the magnetic field, typically between $|B_T|=2.1\,T$ and $2.3\,T$. τ_{ST} is calculated from selected ECE channels laying always inside $q=1$ or, when available, from soft X-ray signals.

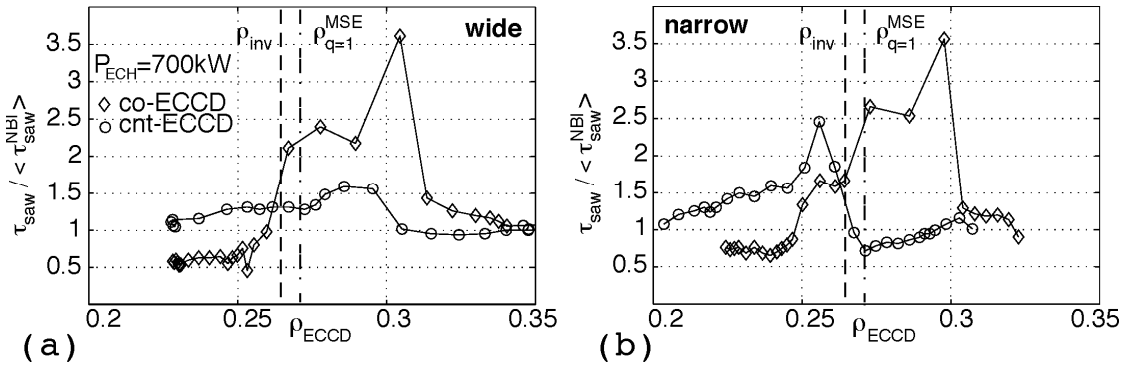

FIGURE 2. Evolution of τ_{ST}, normalised to the period during the NBI-only phase, during ctr- and co-ECCD versus ECCD deposition for (top) wide and (bottom) narrow depositions. The sawtooth inversion radius ρ_{inv} (from ECE) and the q=1 radius $\rho_{q=1,MSE}$ (from MSE) are also plotted.

Figure 2 shows the results of the comparison between the scans in co- and ctr-ECCD for wide and narrow CD depositions [8]. τ_{ST}, normalised to the sawtooth period during the NBI-only phase, is plotted as a function of ρ_{ECCD} (calculated using the beam tracing code TORBEAM [9]). The circles represent measurements during ctr-ECCD, the diamonds during co-ECCD. For comparison, ρ_{inv} (sawtooth inversion radius measured by ECE) and $\rho_{q=1}^{MSE}$ ($q=1$ location measured by MSE) are also shown. The effects of wide and narrow co-ECCD are similar, while the ones of ctr-ECCD are very different. In particular, in the wide ctr-ECCD case, stabilisation of τ_{ST} is observed outside $q=1$, which disagrees with the expectations from the modelling [7]. This is not seen for the narrow ctr-ECCD scan, where on the contrary destabilisation outside and stabilisation inside $q=1$ are measured in accordance with [7]. The reason for this difference is to be attributed to the heating effects: as shown in figure 1, although I_{CD} in the wide deposition case is approximately 30% higher than in the narrow case, $j_{CD}^{\max}$ is on the contrary more than 50% lower than with narrow profile, while the heating effects are basically the same. Hence, comparing the two ctr-ECCD scans clearly indicates that the effects produced by the wide ECCD profiles are dominated by the heating contribution, while the ones produced by the narrow profiles are dominated by the CD contribution. This shows that the narrow deposition is more effective than the wide one and that the driving term for the sawtooth tailoring is not the total driven current I_{CD} but the local driven current density j_{CD}. In addition, $q=1$ is expected to be located at the crossing in sawtooth period between ctr- and co-ECCD. Indeed, the positions of ρ_{inv} and $\rho_{q=1}^{MSE}$ are consistent with the τ_{ST} response to the narrow co- and ctr-ECCD.

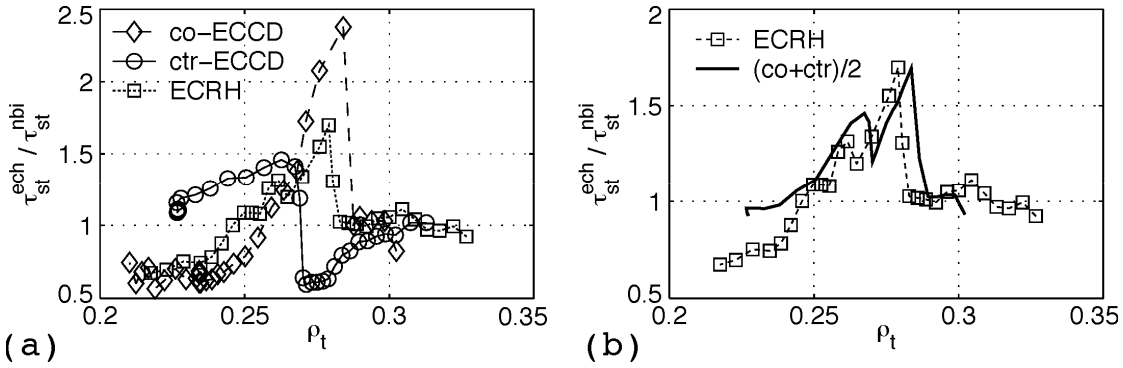

FIGURE 3. (a) τ_{ST} evolution, normalised to the period during the NBI-only phase, during ctr- and co-ECCD, and pure ECRH versus ECCD narrow deposition. (b) Comparison of heating effects between experimental discharge (squares) and calculated from the co-/ctr-ECCD experiments.

To isolate the pure heating effects, an additional experiment has been made in which two gyrotrons at half power have been used, both set for narrow deposition, one in co- and the other in ctr-ECCD at the same location. The two ECCD depositions have been verified using TORBEAM. The idea is that by placing the two sources of CD in opposite direction, but with same total power as for the pure co- and ctr-ECCD, the current drive effects cancel out leaving the heating effects only. The results of these experiments are shown in figure 3. Figure 3 (a) shows the behaviour of τ_{ST} for

the three mentioned cases: co-, ctr-ECCD and pure ECRH using two opposite CD sources. In all cases the total power was $P_{ECRH} = 400\,kW$. The figure clearly shows that the heating effects are in the same direction as the co-ECCD effects, as expected. If we assume linear superposition of the effects of co- and ctrt-ECCD (which seems to be in agreement with the modelling [7]), we can now compare the heating effects on τ_{ST} from the experiment, shown in figure 3 (a), with the heating effects calculated from the co- and ctr-ECCD experiments from which the current drive effects are cancelled out. The calculated sawtooth period is simply obtained from $\tau_{ST}^{calc} = \left(\tau_{ST}^{co} + \tau_{ST}^{ctr}\right)/2$. Figure 3 (b) shows the comparison between the measured and calculated sawtooth period induced by heating only, normalised to the sawtooth period without ECCD. The measured and calculated curves are in very good agreement and support the modelling results, which already indicated such linear behaviour.

NTM CONTROL OPTIMISATION

Once an NTM is triggered, it is of crucial importance to be able to react fast and to stabilise the mode in order to recover from the loss in confinement. For this purpose, a considerable effort has been made in several devices, including ASDEX Upgrade [10-12], DIII-D [13,14] and JT-60U [15]. All the experiments, though, were made with a deposition width d smaller than the marginal island size W_{marg} ($d < W = W_{\mathrm{marg}}$) below which the island decays away independently of β_p. If the island size W is smaller than d, while still being larger than W_{marg} (i.e. if $d > W > W_{\mathrm{marg}}$), theory predicts that the required power can be substantially higher. As for ITER $W_{m\,\mathrm{arg}}$ might be smaller compared to present experiments, this situation could occur and must be tested by artificially achieving $d > W$. If this is the case, theory predicts that a modulation of the ECCD will be required in order to deposit ECCD power only in the O-point of the island [16]. The suppression efficiency as a function of the ratio between W and a modified deposition width d has been investigated both numerically and experimentally for non-modulated ECCD. Toroidal launching angles of the ECRH antennas between 0º (narrowest profile, pure heating) and 25º (broadest CD profile) have been used to vary the CD width and therefore the maximal driven current density and the total driven current I. For large angles, both the current drive efficiency and the deposition width d increase and part of the ECCD current is driven outside the separatrix of the island for $d > W$. This current is lost for the stabilisation of the mode and only $I \cdot W/d$ contributes. This leads to the definition of the figure of merit I/d.

In figure 4 (a), the dashed curve (stars) shows the achievable reduction of the island size due to the ECCD as a function of the toroidal launching angle. The plasma parameters at which the experiments have been performed are the following: $I_P = 800\,kA$, $B_T = 2.0 \rightarrow 2.2\,T$, $P_{NBI} = 10.0\,MW$ and $q_{95} = 5.0$. The island size reduction is normalised to the island size before applying the ECCD, i.e. $W_{\mathrm{norm}} = W_{\mathrm{min}}/W_{\mathrm{sat}}^{\mathrm{noECCD}}$. The straight curve (crosses) shows the calculated driven current normalised to the deposition width, I/d. For small angles (~5º) a clear maximum in I/d is predicted by TORBEAM calculations corresponding to the highest driven current density, although the total driven current increases with the toroidal angle. For angles larger than 15º (broader deposition, reduced I/d), only

partial stabilisation is obtained with typically 1MW of ECCD power. Consistently, with angles between 2º and 15º complete stabilisation is reached ($W_{min}/W_{sat}=0$), both for 1.0MWand 1.4MW of ECCD power. In order to quantify the improvement in stabilisation efficiency, in figure 4 (b) β_N/P_{ECCD} (β_N achieved at the maximum stabilisation normalised to the applied ECCD power) is plotted as a function of I/d. The figure clearly shows that by increasing the driven current density, the NTM stabilisation efficiency is also increased.

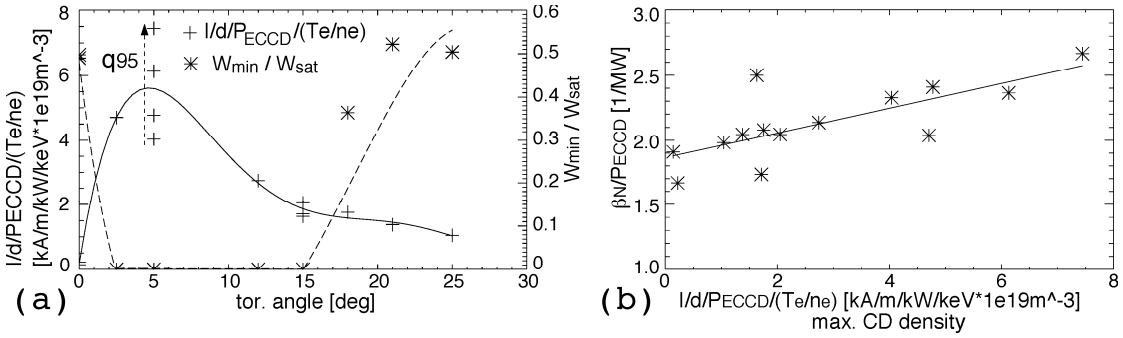

FIGURE 4. (a) Calculated driven current normalised with the deposition width (straight curve, crosses) and normalised island size at maximum stabilisation (dashed curve, stars). (b) NTM stabilisation efficiency in β_N/P_{ECCD} as a function of the normalised driven current I/d.

Based on this scan, the stabilisation scheme has been adopted towards smaller toroidal launching angles with an increased driven current density I/d at the resonant surface. The highest values in achievable β_N and background NBI power are regularly performed with a toroidal angle of 5º. Again, a magnetic field scan is used to target the resonant surface. The stabilisation improvements are summarised in table 1. For the (3/2)-NTM, $\beta_N=2.6$ at $P_{NBI}=12.5\,MW$ and $P_{ECCD}=1.0\,MW$ has been obtained. This increases the achievable ratio between β_N and P_{ECCD} for the (3/2)-NTM to $\beta_N/P_{ECCD}=2.6\,MW^{-1}$. For the (2/1)-NTM stabilisation with increased current density I/d, β_N could be raised from $\beta_N=1.9$ with $P_{NBI}=6.25\,MW$ to $\beta_N=2.3$ with $P_{NBI}=10.0\,MW$ and a reduction of the required ECCD power from 1.9 to 1.4MW. This results for the (2/1)-NTM in $\beta_N/P_{ECCD}=1.6\,MW^{-1}$ compared to originally $\beta_N/P_{ECCD}=1.0\,MW^{-1}$. A further increase of the NBI heating power after the removal of the NTM leads to even higher β_N values as long as the ECCD is preventing another excitation. A new NTM is excited when the ECCD is switched off and a seed island large enough is present.

TABLE 1. NTM stabilization improvement.

NTM	ECCD	q_{95}	P_{NBI} [MW]	β_N	P_{ECCD} [MW]	β_N / P_{ECCD} [MW^{-1}]
(3/2)	cw [wide]	5.0	12.5	2.6	1.20	2.2
(3/2)	mod [wide]	5.0	7.5	2.0	0.55	3.6
(3/2)	cw [narrow]	3.8	12.5	2.6	1.00	2.6
(2/1)	cw [wide]	4.4	6.25	1.9	1.90	1.0
(2/1)	cw [narrow]	4.4	10.0	2.3	1.40	1.6

Most important, as shown in figure 5, is that by reducing the CD deposition width it is now possible to fully stabilise a (3/2)-NTM in ITER-relevant conditions, with low

$q_{95} = 3.8$ [17]. Complete stabilisation was achieved at $\beta_N = 2.7$, with $P_{NBI} = 10.0\ MW$ and $P_{ECCD} = 1.0\ MW$. In the same scenario ($q_{95} = 3.8$), but with wide CD deposition, only partial stabilisation was possible.

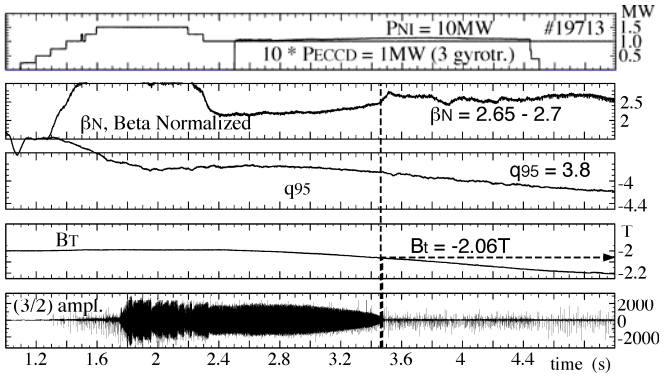

FIGURE 5. Full (3/2)-NTM stabilisation achieved at ITER-relevant q_{95}=3.8 with narrow ECCD deposition and P_{ECCD}=1.2MW.

As mentioned above, if the island size is smaller than the CD deposition width (i.e., if $d > W > W_{m\arg}$), theory predicts that by modulating the ECCD at the mode frequency within the O-point of the island is more efficient than simple cw-ECCD. To validate the theoretical predictions, a series of dedicated experiments with wide ECCD deposition have been performed, once with cw and once with modulated ECCD. To obtain a sufficiently broad ECCD width (for which cw-CD does not stabilise the mode), the toroidal angle has been set to 19º. For the modulated ECCD experiment, it is extremely important to inject the ECCD in phase with the O-point of the island. In order to achieve this requirement, the ECCD power has been modulated at a frequency, and with a phase shift, both calculated using the magnetic pick-up coils. The phase shift has been set up in order to inject the ECCD in the O-point of the island, as well as in the X-point and at the phase for the X-point $\pm 90°$.

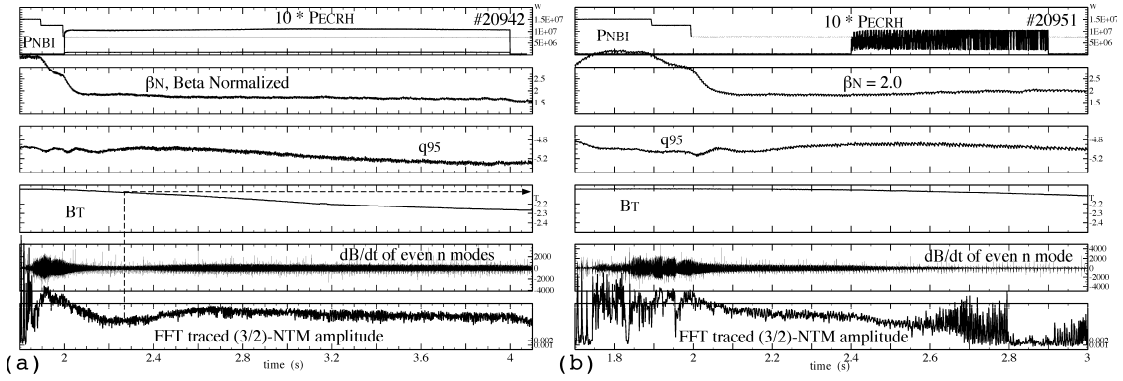

FIGURE 6. (3/2)-NTM stabilisation experiments with wide CD deposition using (a) cw-ECCD and (b) modulated ECCD for the same plasma conditions. While for the cw case the ECCD power is not sufficient to completely stabilise the NTM, using modulated ECCD complete stabilisation is achieved.

Figure 6 shows the comparison of an NTM stabilisation experiment performed with wide CD width. Figure 6 (a) shows the main traces for the case of cw-ECCD, (b) for the case of modulated ECCD. Comparing the (3/2)-NTM amplitude from Fourier transformation of the magnetic pick-up coils (bottom traces) we clearly see that by applying cw-ECCD only a partial reduction of the island is reached, while by applying modulated ECCD full stabilisation is reached. It has to be underlined that the same NTM for the discharge performed with narrow cw-ECCD width is regularly stabilised at much higher β_N.

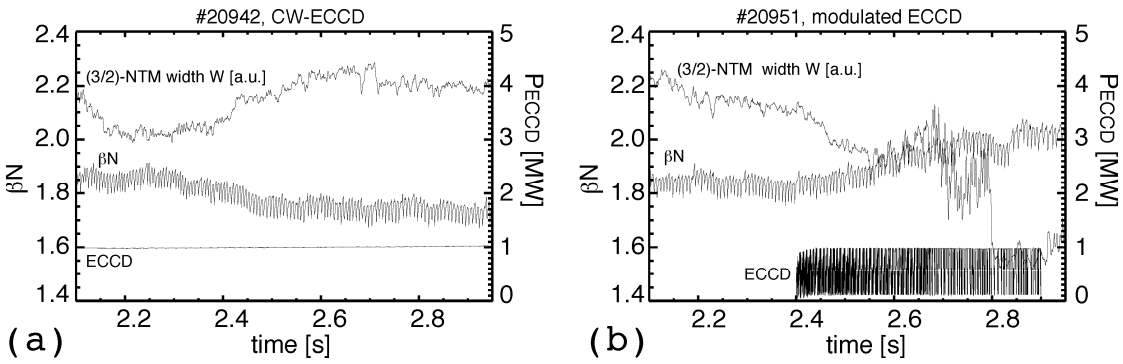

FIGURE 7. (3/2)-NTM stabilisation experiments with wide CD deposition using (a) cw-ECCD and (b) modulated ECCD for the same plasma conditions. Comparison of the behaviour of the NTM island width and of β_N.

Figure 7 shows, for the same discharges as in figure 6, the time evolution of the calculated island size and of β_N. During the magnetic field ramp, non-modulated ECCD reduces only partly the island size, while modulated ECCD completely suppresses the island leading to a recovery of β_N from 1.8 to 2.

CONCLUSIONS

The work presented in this paper aimed at the optimisation of sawtooth and NTM control capabilities by varying the ECRH/CD deposition width, i.e. by varying the driven current density. For the sawtooth control optimisation, comparison of broad and narrow co-/ctr-ECCD and of pure ECRH scans across $q=1$ led to the following results: (i) co-ECCD is more efficient in modifying the sawtooth period than ctr-ECCD; (ii) the strongest effects are obtained with the narrow CD width; (iii) comparing the broad and narrow scans in ctr-ECCD shows that the effects induced on τ_{ST} by the broad CD width are dominated by the heating contribution, while the ones induced by the narrow CD width are dominated by the CD effects; (iv) comparison of the scans in co-/ctr-ECCD with pure ECRH shows that the current drive effects contribute linearly to the modifications of the sawtooth period, in agreement with the modelling results.

For the NTM control studies, a systematic scan of the ECCD deposition width has allowed to significantly increase the NTM stabilisation efficiency, quantified by the parameter β_N / P_{ECCD}. By decreasing the toroidal injection angle of the ECCD, the induced increase in driven current density allowed the extension of the NTM

stabilisation range in q_{95} to ITER relevant conditions. In particular, full stabilisation of a (3/2)-NTM was achieved at $q_{95} = 3.8$ and $\beta_N = 2.7$ with $P_{ECCD} = 1.0MW$, conditions at which no stabilisation is possible with a broad ECCD width. In case of broad ECCD width (larger than the NTM island size) theory predicts that modulated ECCD is more efficient than cw-ECCD. This has been successfully demonstrated for the first time in a plasma with a (3/2)-NTM: by applying cw-ECCD only partial stabilisation at moderate $\beta_N = 1.85$ was possible, while the same discharge performed with modulated ECCD phased to aim at the O-point of the island allowed to reach full stabilisation at a higher $\beta_N = 2.0$ and with half average applied ECCD power. In both scenarios, narrow and broad ECCD width, higher efficiency, expressed in terms of β_N / P_{ECCD}, was reached.

Finally, with respect to ITER and its future launching capabilities, these control optimisation experiments of both sawtooth and NTM clearly indicate that for the purpose of controlling both instabilities, the ECCD deposition profile should be as narrow as possible.

OUTLOOK

For the near future, many tasks are planned in several directions: analysis and modelling, new experiments and hardware development.

For the sawtooth program, the modelling of the sawtooth behaviour during the different ECCD scans, using the Porcelli model [2] implemented into the transport code ASTRA [18], will be performed and the results compared to the experiments. The implementation of the Porcelli sawtooth model in ASTRA is an on-going task in collaboration with the CRPP in Lausanne. On the experimental side, a program on the destabilisation of fast-ion-induced long sawteeth using ECCD has been started. For this task, the fast ion population will be generated using the ion cyclotron resonance heating (ICRH) system of AUG. Then the co-/ctr-ECCD will be scanned across $q = 1$ in order to test the sawtooth control possibilities for ITER-like sawteeth (i.e. sawteeth stabilised by fast ions, in ITER the α-particles generated by the fusion reaction).

For the NTM program, two experiments are on-going. The first one, made in collaboration with the Greek EURATOM Association, plans at trying to avoid the appearance of the modes by applying the ECCD, close to the resonant surfaces, early in the discharge. Comparison experiments between early and late application of the ECCD are planned. In addition, thanks to the optimisation performed for this paper, the goal is to extend the NTM control also to advanced scenarios, typically to the AUG improved H-mode, with the goal of increasing their performance.

Finally, on the hardware side, two more projects are being developed to extend the MHD control capabilities of AUG. On one hand a new ECRH system is presently being installed. Once completed, it will be composed by four gyrotrons, each one of them delivering 1MW of power during 10s. Three gyrotrons will be step-tuneable with four frequencies between 105 and 140GHz, while the first one, which has already been delivered, is a 2-frequency gyrotron at 105 and 140GHz. Each gyrotron will be coupled to independent launching mirrors for which the poloidal angle can be changed during the discharge and the toroidal angle in between shots. Finally, an automatic

feedback system making use of the fast steering possibilities of the poloidal angle is presently under development in collaboration with the IFP in Milano and with the Politecnico di Milano.

ACKNOWLEDGMENTS

We are particularly grateful for the valuable support of the ECRH group of ASDEX Upgrade, without whom this work would not be possible. The main author warmly thanks Clemente Angioni and François Ryter for very fruitful discussions.

REFERENCES

1. O. Sauter et al, *Phys. Rev. Lett.*, **88** 105001 (2002).
2. F. Porcelli et al, *Plasma Phys. Control. Fusion*, **38** p. 2163 (1996).
3. T. G. Goodman et al, *26th EPS Conf. on Controlled Fusion and Plasma Physics*, Maastricht (1999).
4. Z. A. Pietrzyk et al, *Nucl. Fusion*, **39** p. 587 (1999).
5. M. A. Henderson et al, *Fusion Eng. and Design*, **38** p. 2163 (1996).
6. C. Angioni et al, *Nucl. Fusion*, **43** p. 455 (2003).
7. A. Mück et al, *Plasma Phys. Control. Fusion*, **47** p. 1633 (2005).
8. A. Manini et al, *32nd EPS Conf. on Plasma Physics*, Tarragona (2005).
9. E. Poli et al, *Comp. Phys. Comm.*, **136** p. 136 (2001).
10. H. Zohm et al, *Nucl. Fusion.*, **39** p. 577 (1999).
11. G. Gantenbein et al, *Phys. Rev. Lett.*, **85** p. 1242 (2000).
12. G. Gantenbein et al, *30th EPS Conf. on Controlled Fusion and Plasma Physics*, St. Petersburg (2003).
13. R. J. La Haye et al, *Phys. Plasmas*, **9** p. 2051 (2002).
14. C. C. Petty et al, *Nucl. Fusion*, **44** p. 243 (2004).
15. A. Isayama et al, *Plasma Phys. Control. Fusion*, **42** p. L37 (2000).
16. Q. Yu at al, *Phys. Plasmas*, **11** p. 1960 (2004).
17. M. Maraschek et al, *47th APS Conf.*, Denver (2005).
18. G. Pereverzev and P. N. Yushmanov, *ASTRA Automated System for Transport Analysis*, IPP Report 5/98.